Remote Sensing of Environment 113 (2009) 2011–2018

Contents lists available at ScienceDirect

Remote Sensing of Environment

journal homepage: www.elsevier.com/locate/rse

Estimation of evapotranspiration in a mid-latitude forest using the Microwave Emissivity Difference Vegetation Index (EDVI)

Rui Li [a], Qilong Min [a,*], Bing Lin [b]

[a] Atmospheric Sciences Research Center, State University of New York, Albany, NY 12203, United States
[b] Science Directorate, NASA Langley Research Center, Hampton, VA 23681-2199, United States

ARTICLE INFO

Article history:
Received 16 December 2008
Received in revised form 20 May 2009
Accepted 22 May 2009

Keywords:
Evapotranspiration
Forest
Microwave Emissivity Difference Vegetation Index (EDVI)
Diurnal variations

ABSTRACT

We developed an algorithm to estimate evapotranspiration (ET) from dense vegetation covered area from the first principle of surface energy balance model by using satellite retrieved Microwave Emissivity Difference Vegetation Index (EDVI). This algorithm can be used under both clear sky and cloudy sky conditions. Long term seasonal trend of EDVI is linked to variance of canopy resistance due to the interrelationship among leaf development, environmental condition and microwave radiation. Short term changes of EDVI caused by synoptic scale weather variations is used to parameterize the responds of vegetation resistance to the quick changes of environmental factors including water vapor deficit, water potential and others. The performance of this algorithm was test at the Harvard forest site by using satellite measurements from the SSM/I F13 and F14 sensors. Validation at the site with 169 samples shows that the correlation coefficient (R^2) between estimated and observed ETs is 0.83 with a mean bias of 3.31 Wm^{-2} and a standard deviation of 79.63 Wm^{-2}. The overall uncertainty of our ET retrieval is ~30%, which is within the uncertainty of current ground based ET measurements. Furthermore, the estimated ET in different local times (up to 4 times per day) successfully captured the diurnal cycle of ET. It is the first time that the diurnal variations of vegetation–atmosphere interactions were directly monitored from space. This study demonstrates that the technique reported here extends the current satellite capability of vegetation property and ET flux remote sensing from daytime, clear-sky conditions to day and night times and from intermediate leaf area index (LAI) to all range of vegetation states.

Published by Elsevier Inc.

1. Introduction

An accurate depiction of evapotranspiration (ET) and photosynthesis processes is essential in the understanding of the response and influence of the vegetation system to water, energy, and carbon cycles of the climate (Huntingford et al., 2005; O'Brien, 1996; Shukla & Mintz, 1982; Shukla et al., 1990; Wang et al., 2009; Zeng et al., 1999), which requires monitoring vegetation–atmosphere interactions in all weather conditions. ET (or land surface latent heat) processes are associated with many complicated physical and biological phenomena such as turbulence, energy, moisture, and vegetation state. Land surface and meteorological conditions determine the partitioning of surface available energy to the sensible heat flux and latent heat flux. Consequently, these land surface fluxes influence the timing and evolution of cumulus convection, in particular, the cloud base height and depth as well as convective available potential energy. Thus, a feedback loop is formed in the atmospheric–terrestrial system in terms of water and energy cycles even at very short temporal and small spatial scales.

Although clouds are intrinsically linked to climate variability, their effect on surface-atmosphere exchange on long temporal (inter-annual) and large spatial (regional to global) scales has received relatively little attention. Because of enhanced ET and carbon uptake under moderate cloudy skies, an understanding of vegetation–atmosphere feedback for all weather conditions is critical (Min, 2005; Min & Wang, 2008). Furthermore, the wide spectra of spatial and temporal scales of the climate system and inherent heterogeneity of the biosphere require the use of remote sensing techniques to study and monitor surface/canopy states, their related atmospheric and environmental change processes, and the effects of variations in vegetation on large scale atmospheric dynamics and thermodynamics.

Ground-based flux towers provide relatively accurate "point" measurements of ET. However, to project these measurements to larger landscape area will certainly introduce large errors. Satellite remote sensing is the most feasible way to solve this problem. Existing satellite remote sensing techniques for ET estimations are mainly based on measurements at visible and near-infrared wavelengths, such as normalized difference vegetation index (NDVI), enhanced vegetation index (EVI) and Normalized Difference Water Index (NDWI)—spectral

* Corresponding author.
E-mail address: min@asrc.cestm.albany.edu (Q. Min).

0034-4257/$ – see front matter. Published by Elsevier Inc.
doi:10.1016/j.rse.2009.05.007

measurements that are correlated to the absorbed fraction of photosynthetically active radiation (PAR) and water. Nishida et al. (2003) developed a potentially-operational ET estimation algorithm based on surface energy balance (SEB) model of two surface types (bare soil and vegetation). NDVI derived from MODIS was used to determine the partition of vegetated area. However, these optical vegetation indexes have some limitations: 1) low temporal resolution caused by high sensitivity to clouds and aerosols and unable to provide information under cloudy conditions; and 2) saturation at intermediate values of leaf area index (LAI) (Asrar et al., 1984; Granger, 2000; Gutman, 1999; Myneni et al., 1995; Sellers, 1985). Because of the rapid change of vegetation state during spring onset and fall senescence, these indexes cannot accurately capture the transitions of vegetation states during growing seasons. In some regions where cloud covers are high, for example in Amazon Basin, these indexes are inadequate to provide information of the structure and function of terrestrial ecosystems, particularly in rainy seasons. Thus, there are considerable gaps in the understanding of feedback mechanisms associated with atmosphere–terrestrial ecosystem exchange and hydrological cycle.

To overcome the above limitations, Min and Lin (2006a,b) have developed a novel technique that links vegetation properties and ET with an "Emissivity Difference Vegetation Index" (EDVI), defined as the microwave land surface emissivity (MLSE) differences between two wavelengths. These EDVI values are derived from a combination of satellite microwave measurements and visible and infrared observations. This technique is applicable under all-weather conditions for monitoring vegetation biomass and ecosystem exchange processes, particularly under cloudy conditions favorable to surface–atmosphere exchange. By combining EDVI measurements with classic satellite indexes of vegetation at visible and near-infrared wavelengths, continuous daily global operational measurements of canopy properties will be possible. Min and Lin (2006a) have demonstrated there is a good correlation between the measure ET fraction and EDVI. In this study, we develop a quantitative algorithm to estimate evaporation fraction (EF, the ratio of ET to available energy) and ET by using the high temporal resolution of EDVI and validate the retrievals with tower measurements at the Harvard forest site.

2. Measurements and retrieval algorithm of ET

The Harvard Forest Environmental Monitoring Station (EMS) is located in north central Massachusetts (42.54 °N, 78.18 °W). The forest is 50–70 years old and contains a mixture of red oak, red maple, and hemlock with an average tree height of 24 m. Since the coverage of forest at Harvard Forest is very high and fairly homogeneous during grown seasons, it is reasonable to assume that the ET is mainly contributed by vegetation and to neglect the evaporation from soil moisture. The site has been equipped with a suite of radiation and turbulent flux measurements since 1991 (Moore et al., 1996; Wofsy et al., 1993). The net radiation (R_N), ground heat flux (G), PAR, land surface fluxes including sensible heat, water vapor and CO_2, and corresponding meteorological state variables (temperature, pressure, humidity, wind etc.) in 30-minute temporal resolution are used for parameterization and for validation. Daily mean precipitation data are also used to discuss the impact of rain on ET estimation.

2.1. EDVI and normalized EDVI

The optical depth at microwave wavelengths has a semi-empirical linear relationship with vegetation water content (VWC) and varies systematically with both wavelength and canopy structure (Jackson & Schmugge, 1991). The microwave emissivity difference between two wavelengths minimizes the influence of the soil emission underneath vegetation canopy and is sensitive to VWC and other vegetation properties between two emission layers in different effective thickness. Min and Lin (2006a) proposed a new vegetation index: microwave emissivity difference vegetation index, based on the microwave land surface emissivity difference between two wavelengths to indicate VWC and other vegetation properties of the canopy. The EDVI is defined as:

$$\mathrm{EDVI}_P = \frac{\mathrm{MLSE}_P^{19} - \mathrm{MLSE}_P^{37}}{0.5\left(\mathrm{MLSE}_P^{19} + \mathrm{MLSE}_P^{37}\right)} \tag{1}$$

where p represents a polarization at vertical or horizontal direction. 19 and 37 indicate 19.4 GHz and 37.0 GHz channels of microwave measurements of SSM/I, respectively. This normalized emissivity difference further minimizes its dependency on canopy skin temperature (i.e. the thermodynamic temperature of leaf surface) and thus substantially reduces its uncertainty when canopy skin temperature retrievals are problematic under cloudy conditions.

Detailed retrieval algorithm and its application have been discussed in Min and Lin (2006a,b). Here we briefly sketch the retrieval process of EDVI for the SSM/I data from the Defense Meteorological Satellite Program (DMSP) F13 and F14 satellites from 1999 to 2000 at the Harvard Forest site. For all SSM/I wavelengths and polarizations, MLSE values are estimated based on an atmospheric microwave radiative transfer (MWRT) model (Lin & Minnis, 2000; Lin et al., 1998), which accurately accounts for the atmospheric absorption and emission of gases and clouds, especially the temperature and pressure dependences of these radiative properties (Lin et al., 2001). Only non-precipitating cases were analyzed to avoid the complexity of microwave scattering and the dependence of observed radiances on precipitating hydrometeors. The major inputs for the retrieval are effective land surface skin temperature, column water vapor (CWV), cloud water amount, surface air temperature and pressure. The European Center for Medium-range Weather Forecasts (ECMWF) assimilation data is used to estimate CWV values. Atmospheric optical depths inferred from total shortwave measurements assuming 8 μm cloud droplet effective radius were converted to cloud water amount. The vertical distributions of atmospheric temperature, pressure and gas abundance were constructed based on climatological profiles (McClathey et al., 1972) and interpolated to conform to the surface measurements of temperature and pressure and ECMWF CWV values. Since the coverage of forest at Harvard Forest within the footprint of 19 GHz channels (69×43 km^2, the largest of SSM/I) is very high, the possible heterogeneity contribution of forest to the emissivity is minimal. As indicated by Min and Lin (2006a), the vertical component of the EDVI has a higher correlation with the evapotranspiration than the horizontal component. We use the vertical component of EDVI in this study.

Further as outlined in Min and Lin (2006b), we define a normalized EDVI_V to quantify the leaf development stage as:

$${}^{N}\mathrm{EDVI} = \frac{\mathrm{EDVI} - \mathrm{EDVI}^{\mathrm{onset}}}{\mathrm{EDVI}^{\mathrm{max}} - \mathrm{EDVI}^{\mathrm{onset}}} \tag{2}$$

where $\mathrm{EDVI}^{\mathrm{onset}}$ and $\mathrm{EDVI}^{\mathrm{max}}$ are EDVI at the spring onset and the maximum EDVI during the growing season, respectively. The ^{N}EDVI is the relative change of EDVI from its spring onset value during a growing season and represents well the leaf growing stage during the growing season (Min & Lin, 2006b).

Fig. 1 shows EDVI retrievals from SSM/I on board FM13 and FM14 satellites under both clear sky conditions and cloudy conditions. For certain periods, by combining two satellite overpasses, we are able to get a high temporal resolution of EDVI, up to 4 values per day at four local times of around 5am, 9am, 4pm and 8pm. Such daily multiple observations provide a possibility to monitor diurnal variation of vegetation states and associated ET. Certainly, the temporal resolution can be further improved when retrievals in rain conditions are available, and by combining other multiple-channel microwave sensors such as TRMM Microwave Imager (TMI) and Advanced Microwave Scanning Radiometer–EOS (AMSR–E).

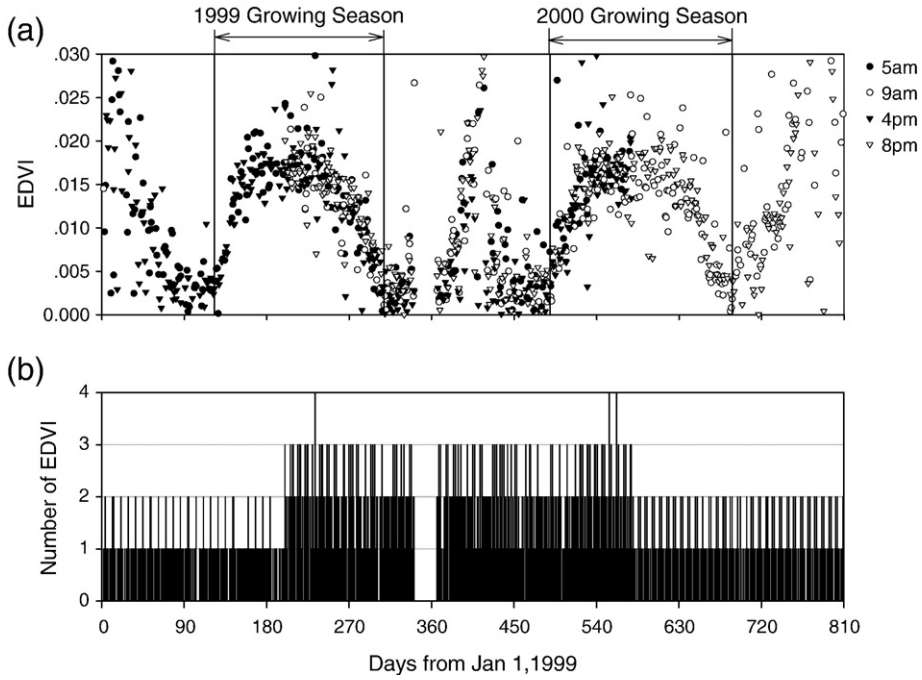

Fig. 1. Time series of EDVI in high temporal resolution and the daily sample numbers from 1999 to 2000.

EDVI is influenced by land surface properties including properties of vegetation, soil, and snow. Based on studies of Min and Lin (2006a,b), EDVI during the growing season is closely related to the vegetation properties: such as leaf development stages, vegetation water content, etc. During the winter or other seasons, however, EDVI is sensitive to the snow pack and soil conditions. In this study, we only focus on retrievals during growing seasons. The variations of EDVI during a growing season can be divided into two components. The first is a "slow" variation that is represented by the normalized EDVI. Min and Lin (2006b) demonstrated that the normalized EDVI is a good indicator of vegetation development states. We use this slow variation component to parameterize the minimal canopy resistance. The second is a "quick" variation component, which represents the day-to-day variations during the growing season. We consider that such variation is mainly contributed by the stress of environmental factors. Although "precipitating" cases are excluded, the intercepted water on the leaf surface from rain events can be incorrectly regarded as vegetation water, resulting in overestimates of EDVI and consequently ET.

2.2. Retrieval algorithm of ET

The ET processes depend upon the availability of both water within the soil and canopy and energy to change the water state along with forest–atmosphere dynamics. The net energy exchange is a function of environmental factors such as incoming radiation, which shows large diurnal changes responding to variations in the solar zenith angle and cloud coverage. To understand the linkage of ET fluxes to surface properties, some studies have used the evaporation fraction (EF) as an index for ET (Jiang & Islam, 2003; Nishida et al., 2003; Shuttleworth et al., 1989):

$$\mathrm{EF} = \mathrm{ET} / (R_N - G) \tag{3}$$

where R_N and G are the net radiation and the ground heat flux, respectively. Since EF is nearly constant during daylight hours (Crago, 1996; Shuttleworth et al., 1989), it can be used for scaling instantaneous satellite observations to longer time periods (daily or daytime). Moreover, EF is directly related to the surface energy partition or Bowen Ratio (BR) by $\mathrm{EF} = 1/(1+BR)$.

In reality, ET of forest ecosystem is composed of transpiration of vegetation and evaporation from bare soil and intercepted precipitation. Since the coverage of forest at Harvard Forest within the footprint of 19 GHz channels (69×43 km^2, the largest of SSM/I) is very high, and EDVI is not retrieved under rainy conditions, we simply ignored the latter two terms in the current study. However, the possible errors or uncertainties introduced by these effects will be discussed later. The linkage between vegetation EF and the canopy and aerodynamic resistance can be described as (Nishida et al., 2003):

$$\mathrm{EF} = \frac{\alpha \Delta}{\Delta + \gamma(1 + r_C / r_a)} \tag{4}$$

α is the Priestley–Taylor's parameter ranging from 1.1 to 1.4 (Monteith, 1995; Priestley & Taylor, 1972). Δ is the derivative of the saturated vapor pressure against temperature (Pa/K). γ is the psychometric constant (Pa/K). r_a is aerodynamic resistance (s/m) determined by wind speed, while r_c is the vegetation canopy resistance. To determine those parameters we need to know not only vegetation states but also the corresponding meteorology parameters including temperature, pressure, humidity and wind in boundary layer. Directly obtaining some of those parameters from satellite remote sensing is still challenging, but steady advances have been made recently (Hashimoto et al., 2008; Nishida et al., 2003; Njoku & Li, 1999). Temperature, pressure, humidity and wind in boundary layer, except r_c, at least, can be readily obtained from re-analysis with adequate accuracy. As a non-operation algorithm and for illustrating retrieval capability, we simply use the in-situ measurements from the meteorology station at the site.

In Eq. (4), the most important unknown parameter is the vegetation canopy resistance r_c, which is a function of vegetation and environmental states. In general, the canopy resistance consists of two parts: the cuticle resistance and the stomatal resistance. Based on the classical Javis-type equation, we have:

$$\frac{1}{r_c} = \frac{f_1(Ta) f_2(\mathrm{PAR}) f_3(\mathrm{VPD}) f_4(\Psi) f_5(\mathrm{CO_2})}{r_{\mathrm{cmin}}} + \frac{1}{r_{\mathrm{cuticle}}} \tag{5}$$

The stomatal resistance is expressed as a product of a minimal resistance, r_{cmin}, and the stress functions (f_1 to f_5) associated with

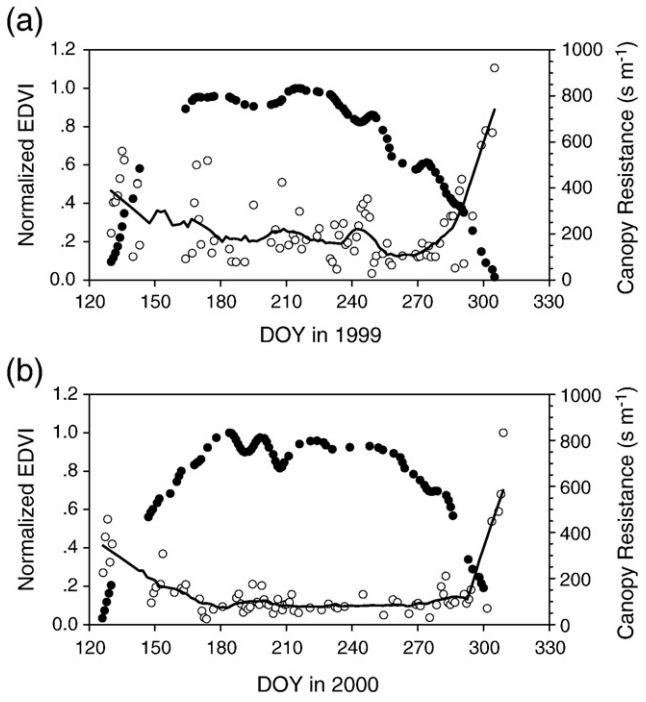

Fig. 2. Time series of normalized EDVI (solid circles) and canopy resistance (opened circles) in Harvard Forest during the growing seasons of 1999 and 2000.

environmental states, such as air temperature, T_a, photosynthetic active radiation PAR, water vapor pressure deficit VPD, water potential ψ, and ambient carbon dioxide concentration CO_2. We set the cuticles resistance, $r_{cuticle,}$ to be 10^5 sm^{-1}. In this study, however, we directly connect some of these parameters with our retrieved EDVI, as EDVI represents vegetation states.

The minimal canopy resistance r_{cmin}, a resistance without any environmental stress, is largely determined by the vegetation states. The more the leaf developed in the canopy the smaller the canopy resistance would be. As demonstrated by Min and Lin (2006b), the EDVI is sensitive to leaf development through vegetation water content of the crown layer of the forest canopy, and the leaf growing stage can be monitored accurately by the normalized EDVI (^{N}EDVI). Fig. 2 shows ^{N}EDVI for the growing seasons of 1999 and 2000 and the corresponding canopy resistance that is derived from in situ measured latent heat flux measurements and associated meteorology. After the spring onset in both 1999 and 2000, ^{N}EDVI increased quasi-linearly in the first 20 days accompanied by leaf emergence and reached its maximum a month later. In the meantime, the smoothed canopy resistance decreased accordingly. During the steady state of the growing season, the canopy resistance stayed in small values with a minimum value of about 17 sm^{-1}, while the ^{N}EDVI varied closely to its maximum. As the ripening process proceeds with leave drying up and consequently falling, ^{N}EDVI decreased gradually to a small value before LAI to decrease (Min & Lin, 2006b). Changes in VWC and LAI result in the canopy resistance to increase to a large value. It is clear that the canopy resistance is generally anti-correlated with ^{N}EDVI, which represents the vegetation development states. The canopy resistance is controlled not only by the minimal canopy resistance, but also by the stress of many environmental factors. ^{N}EDVI indicates the vegetation water content in the canopy, which is more important than the leaf amount for photosynthesis and vegetation–atmosphere interaction processes. Therefore, the minimal canopy resistance is assumed to be:

$$r_{cmin} = r_{cmin0} / {}^N\mathrm{EDVI} \tag{6}$$

where r_{cmin0} is the baseline of the minimum canopy resistance, representing vegetation characteristic at the site. From the canopy resistance derived from the measurements at Harvard forest, we set r_{cmin0} to be 17 sm^{-1}. Eq. (6) basically assumes that the variation of the minimum canopy resistance during growing season is dependent on the vegetation state parameter ^{N}EDVI. It is worth noting that the traditional optical vegetation index with sparse temporal resolution and possible saturation problem cannot accurately capture the transitions of vegetation states during growing seasons. Such that most NDVI based algorithms do not account for the variation of vegetation states during the growing season.

Environmental stresses further regulate the canopy resistance. Since air temperature and PAR are readily obtained from satellite observation, we directly account for both variables and adopted the function forms of f(Ta) and f(PAR) from Jarvis (1976) and Kosugi (1996):

$$f_1^{(Ta)} = \left(\frac{T_a - T_n}{T_0 - T_n}\right)\left(\frac{T_x - T_a}{T_x - T_a}\right)\left[\frac{Tx - T0}{T0 - Tn}\right] \tag{7}$$

$$f_2(\mathrm{PAR}) = \frac{\mathrm{PAR}}{\mathrm{PAR} + A}$$

where parameters T_n, T_0 and T_x are minimum, optimal and maximum temperatures for stomatal activity. Parameter A is related to efficiency of photon absorption and set to be 152 (Nishida et al., 2003).

Direct measure of VPD, water potential, ψ, and ambient carbon dioxide concentration of functions f_3, f_4, and f_5, respectively, from satellites is very challenging. Some remote sensing algorithms of ET simply set the functions of f_3, f_4, and f_5 to be 1 (Nishida et al., 2003). As discussed previously, the slow variation of EDVI represents changes in vegetation state, determined by seasonal dynamics of vegetation at the geo-location. There are still significant day-to-day and even diurnal variations of EDVI, shown in Fig. 1. Within 24 h, particularly in the steady state of a growing season, changes in the leaf development/amount are very small and the fast variation of EDVI represents canopy response to the changes of environmental conditions, such as VPD, water potential and carbon dioxide concentration. Increase of EDVI in daily or diurnal scales indicates increase of VWC, which could be due to water recharge through vegetation roots and/or intercept of water on leaves. Water recharge could result in lower water potential, and intercept water will result in lower VPD. As shown in Fig. 3a, there is a fair correlation between the day-to-day variations of EDVI, dEDVI, and the changes of VPD, dVPD, with correlation coefficient of 0.47. Those non-raining samples (39 pairs) used here were at least two consecutive days with valid observations. The scattering of the dVPD–dEDVI relationship indicates the fact that there are more factors other than VPD can impact the value of EDVI. More interestingly, shown in Fig. 3b, the ratio of two consequent samples of combined $f_{3,4,5}$ (removing the impacts of $f_1(T_a)$ and f_2 (PAR)) is correlated with dEDVI ($R = 0.56$, 69 s maples), indicating better representative of EDVI for the combination of the rest three stress functions. Hence, we can parameterize $F_{3,4,5,}$ based on the difference between the EDVI and the baseline EDVI^S (smoothed EDVI), as

$$F_{3,4,5} = f_3(\mathrm{VPD}) f_4(\Psi) f_5(CO_2) = \left[1.186 - 105.755\left(\mathrm{EDVI} - \mathrm{EDVI}^S\right)\right]^{-1} \tag{8}$$

Eqs. (3)–(8) represent our basic retrieval algorithms of EF and ET. Parameters listed in those equations are either directly obtainable from satellite remote sensing or from re-analysis.

3. Results

In the following, we will use EDVI combined with some surface measurements to demonstrate and validate our retrievals. FM13 and FM14 satellites passed over Harvard forest site at around 9 am and

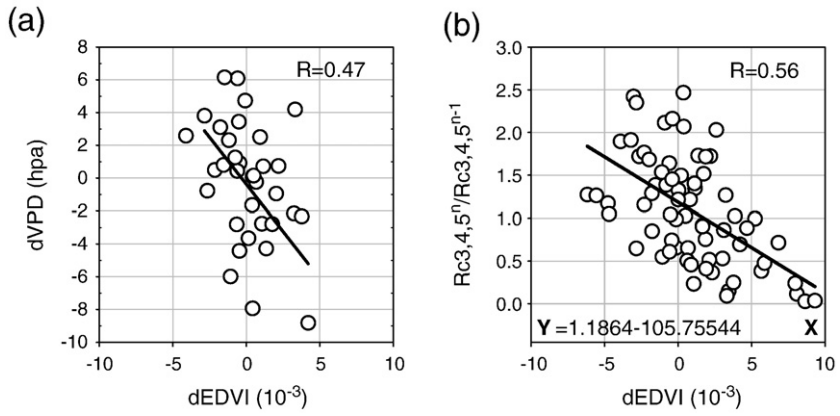

Fig. 3. Correlations between (a) day-to-day variations of VPD (dVPD) and EDVI (dEDVI); (b) day-to-day variations of *Rc*3,4,5 (ratio) and EDVI (dEDVI).

4 pm local times during daytime. We retrieve both EF and ET at corresponding morning and afternoon overpasses and also estimate daily average EF and ET by combined retrievals from both morning and afternoon overpasses. Fig. 4 shows direct comparison between observed and estimated ET and EF for both growing seasons of 1999 and 2000. The retrieved EF captures the seasonal variation very well

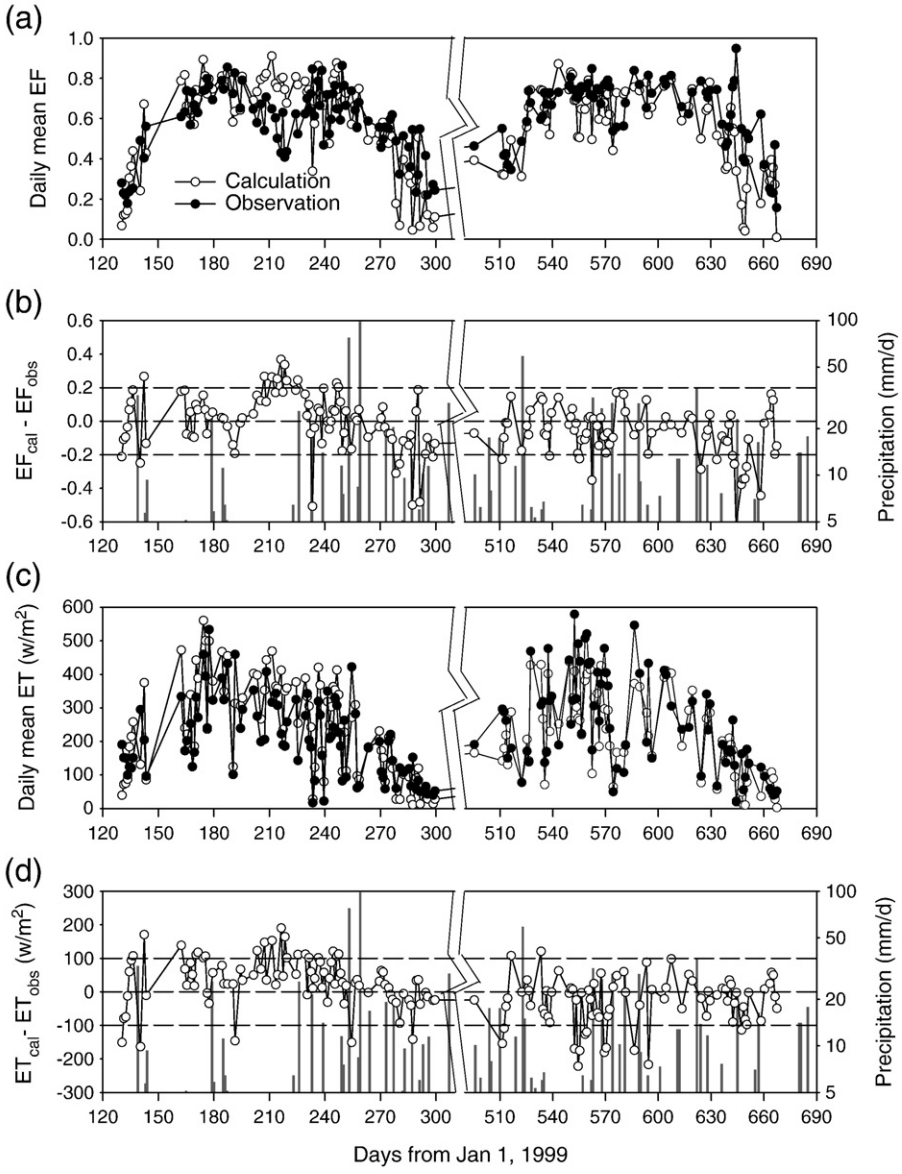

Fig. 4. Time series of observed and calculated daily mean EF, ET and the differences between them. Observed daily precipitation (>5 mm/day, gray bars) is also shown.

in the transient periods and during the steady state of the growing season. It implies that the normalized EDVI could represent the seasonality of vegetation state, providing an accurate assessment of minimum canopy resistance in the entire growing season. With observed available energy, it is easy to derive ET from retrieved EF, shown in Fig. 4c. ET has larger variation due to additional variability of available energy. Estimated ET agrees with observed ET, even at short time scales. With high temporal resolution of retrieved EDVI, we are able to derive temporal variation of EF and ET from satellite remote sensing caused by synoptic scale weather systems, which is important for understanding vegetation–atmosphere interaction. Such information is not readily obtained from traditional retrievals based on 8-day or 16-day composited optical vegetation indexes.

Most differences between estimated and observed EF are smaller than 0.2, shown in Fig. 4b. Some large negative differences do occur and are strongly related to precipitation. In this study, we did not separate evaporation from transpiration. Although we excluded days with rainfall that can be directly detected by satellite, precipitation which occurred before and after satellite overpasses may enhance water availability through soil and leaf interception. Evaporation of intercepted water would enhance EF and ET. Without considering evaporation process the current algorithm will result in a negative bias in estimated EF and ET due to the influence of precipitation. Further, most differences between estimated ET and observed ET are smaller than 100 Wm^{-2} and some larger differences are mainly associated with precipitation.

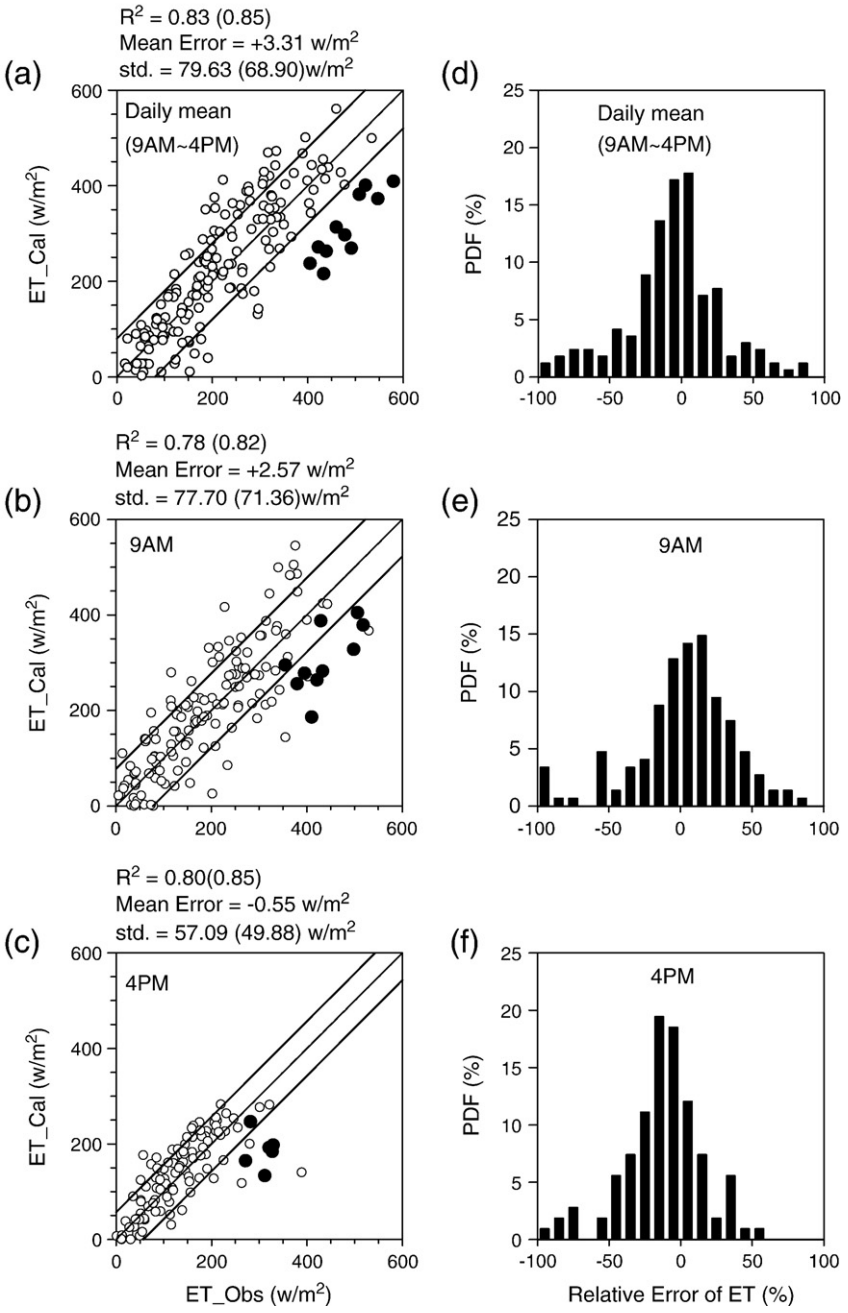

Fig. 5. Estimated and observed ET at daily mean (9am–4pm), 9am and 4pm and the distribution of the relative error. The three straight lines in each plot are the 1:1 line and that ± 1 standard deviation of observation, respectively. Solid circles are those samples severely contaminated by precipitation. New statistics of ET estimation excluding those samples are filled in parenthesis.

Statistically, as shown in Fig. 5, the correlation coefficient (R^2) between estimated and observed ETs is 0.83 with a mean bias of 3.31 Wm^{-2} and a standard deviation of 79.63 Wm^{-2}. If we excluded the data that may be influenced by precipitation, the standard deviation is further reduced to 68.90 Wm^{-2} with a better correlation coefficient (R^2) of 0.85. We should emphasize that observational uncertainties are considerable. The footprint of tower flux measurements is only a small fraction of footprints of SSM/I sensors. Scale-inconsistencies have certain effects on the evaluation and comparison of the satellite and surface data. Uncertainties associated with ground observations of ET fluxes are also large. Small errors in meteorological variable measurements may produce non-negligible errors in these fluxes (i.e. Section C in Glenn et al., 2007 and related literatures therein). Overall, the mean difference between estimated and observed ET is ~30%, which is within the uncertainty of current ground based ET measurements (20%–30%, Glenn et al., 2007). These statistical characteristics indicate that this retrieval algorithm is comparable or better than most existing retrieval algorithms, particularly for retrievals under both clear-sky and cloudy conditions (Glenn et al., 2007).

Fig. 5 also shows the comparison of observed and estimated EF and ET at satellite overpass times of 9am and 4pm. For the morning overpass retrievals, the estimated ETs have a mean error of 2.57 Wm^{-2} and a standard deviation of 77.70 Wm^{-2} with a correlation coefficient (R^2) of 0.78. For the afternoon overpass retrievals, the estimated ETs have a mean error of −0.55 Wm^{-2} and a standard deviation of 57.09 Wm^{-2} with a correlation coefficient (R^2) of 0.80. There are even better accuracies for both morning and afternoon overpasses, if the precipitation contaminated data are removed.

Precipitation not only impacts on EDVI retrievals due to hydrometeor scattering but also introduces a large error of ET estimation after precipitation events due to uncertainties of intercepted water processes. Retrievals of ET with weekly accumulated precipitation larger than ~20 mm have remarkable negative mean errors of −151.37 w/m^2 and −125.88 w/m^2 at 9am and 4pm, respectively. These errors are 2–3 times larger than the associated overall standard deviations (77.70 w/m^2 at 9am and 57.09 w/m^2 at 4pm). It illustrates the significant impacts of precipitation on ET estimation.

Overall good agreement between estimated and observed ET for both morning and afternoon satellite overpasses demonstrates a great opportunity to monitor diurnal variation of vegetation state, EF, and ET using daily multiple-overpass measurements of satellites. For example, as shown in Fig. 1, by combining SSM/I measurements from FM13 and FM14 satellites, we are able to get up to 4 measurements daily. To demonstrate this capability, we chose all days that had three or four satellite overpasses to retrieve EDVI and estimate ET (about 30 samples with three overpasses and 3 samples with four overpasses). To illustrate the diurnal cycle of ET, we averaged observed ET for those days, shown in Fig. 6. EDVI was high (0.0171) at dawn (~5am), due to high VWC through water recharge process at night. The EDVI deceased throughout the day (0.0160 at 9am and 0.0157 at 4pm) as

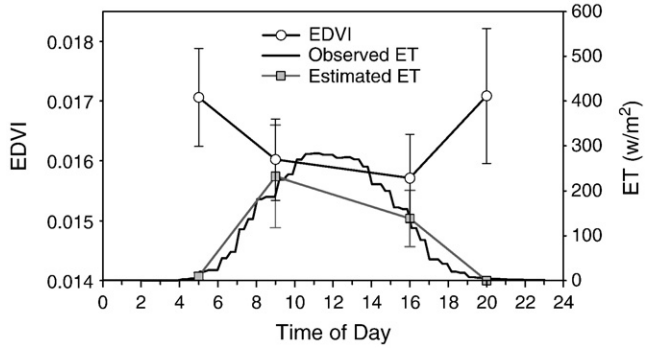

Fig. 6. Diurnal cycle of EDVI, estimated ET (Wm^{-2}) and the in-situ observed ET (Wm^{-2}).

the evapotranspiration process extracted water from vegetation. Late into the night, with diminishing of evapotranspiration process, water recharge process uptakes water from root to the leave and branches, resulting in a high EDVI value. Applying the diurnal cycle of EDVI, the estimated ET increases from 9.43 ± 8.54 Wm^{-2} at 5am to 232.23 ± 114.21 Wm^{-2} at 9am, and then decreases to 138.57 ± 62.89 Wm^{-2} at 4pm and to 0.00 at 8pm due to changes of available energy at that time. The diurnal cycle of estimated ET agreed well with averaged measurements of ET. Although there are only four samples of EDVI and ET per day, those retrievals reasonably reflect the diurnal cycle of vegetation properties and ET. Combining with other multiple-channel microwave sensors, such as TMI and AMSR–E, it will certainly enhance observational frequencies and better remotely sense the diurnal cycle of vegetation states and ET.

4. Conclusion

We have developed a novel technique that links vegetation properties and ET fluxes with an "emissivity difference vegetation index", defined as the microwave land surface emissivity (MLSE) differences between two wavelengths (Min and Lin, 2006a,b). These EDVI values are derived from a combination of satellite microwave (MW) measurements with visible and infrared observations. Taking advantage of high temporal resolution of EDVI, we developed an algorithm to estimate EF and ET from the first principle of surface energy balance model. The slow variation of EDVI, represented by the normalized EDVI, provides an accurate measure of vegetation state during the growing season, and thus is used to scale the minimal canopy resistance. As EDVI is directly linked to VWC, the fast changes of EDVI represents canopy response to the changes of environmental conditions, such as VPD, water potential (and carbon dioxide concentration). It allows us to parameterize the combined stress functions of environmental factors of VPD, water potential, and carbon dioxide concentration. Utilizing both slow and fast variations of retrieved EDVI, we are able to accurately estimate canopy resistance, and thus EF.

From direct comparison with the in-situ observation of EF at the Harvard Forest site, the estimated EF from our retrieval algorithm captures not only the seasonal variation in the transient periods and during the steady state of the growing season but also temporal variation of EF caused by synoptic and diurnal weather changes. Such information is not readily obtained from traditional retrievals based on 8-day or 16-day composited optical vegetation indexes. With observed available energy, it is easy to derive ET from retrieved EF. Validation at the site shows that the correlation coefficient (R^2) between estimated and observed ETs is 0.83 with a mean bias of 3.31 Wm^{-2} and a standard deviation of 79.63 Wm^{-2}. The overall mean difference of our ET retrievals with in-situ measurements is ~30%, which is within the uncertainty of current ground based ET measurements and comparable to most existing retrieval algorithms (Glenn et al., 2007). It is worth noting that the above statistics include retrievals under both clear-sky and cloudy conditions. The results of this study were obtained over a dense forest cover limited to the growing season period. We speculate that our method is applicable under all-weather conditions and extends current satellite remote sensing capability of vegetation properties and ET fluxes from daytime, clear-sky conditions to day and night times and from intermediate LAI to all range of vegetation states. Extensive application of this method to different vegetation regimes is under way. Although the present version of this algorithm is running on an off-line mode, our aim is to develop an operational algorithm in estimating ET from a combination of satellite microwave measurements with visible and infrared observations. Currently, our physically-based EF retrieval algorithm has three basic modules: meteorological conditions, radiation, and EF. All key inputs for the three modules of this algorithm can be replaced by satellite remote sensing and reanalysis data. For

examples, the surface net radiation income (R_N) and the photosynthetic active radiation can be retrieved from the combined observations of Clouds and Earth's Radiation Energy System and the Moderate Resolution Imaging Spectroradiometer. The upgraded operational technique for EF and ET estimations will be a unique tool in studying the atmospheric water and energy cycle and vegetation–atmosphere interactions at diurnal, synoptic and climate scales.

Acknowledgments

This research was supported by the Office of Science (BER), U.S. Department of Energy, Grant DE-FG02-03ER63531, and by the NOAA Educational Partnership Program with Minority Serving Institutions (EPP/MSI) under cooperative agreements NA17AE1625 and NA17AE1623.

References

Asrar, G., Fuchs, M., Kanemasu, E. T., & Hatfield, J. L. (1984). Estimating absorbed photosynthetic radiation and leaf area index from spectral reflectance in wheat. *Agronomy Journal*, *76*, 300—306.

Crago, R. D. (1996). Comparison of the evaporative fraction and the Priestley–Taylor for a parameterizing daytime evaporation. *Water Resources Research*, *32*, 1403—1409.

Glenn, E. P., Huete, A. R., Nagler, P. L., Hirschboeck, K. K., & Paul, B. (2007). Integrating remote sensing and ground methods to estimate evapotranspiration. *Critical Reviews in Plant Sciences*, *26*, 139—168.

Granger, R. J. (2000). Satellite-derived estimates of evapotranspiration in the Gediz basin. *J. Hydrology*, *229*, 70—76.

Gutman, G. G. (1999). On the use of long-term global data of land reflectances and vegetation indices derived from the advanced very high resolution radiometer. *Journal of Geophysical Research*, *104*(D6), 6241—6255.

Hashimoto, H., Dungan, J. L., White, M. A., Yang, F., Michaelis, A. R., Running, S. W., et al. (2008). Satellite-based estimation of surface vapor pressure deficits using MODIS land surface temperature data. *Remote Sensing of Environment*, *112*, 142—155.

Huntingford, C., Lambert, F. H., Gash, J. H. C., Taylor, C. M., & Challinor, A. J. (2005). Aspects of climate change prediction relevant to crop productivity. *Philosophical Transactions of the Royal Society of London B*, *360*, 1999—2009.

Jackson, T. J., & Schmugge, T. J. (1991). Vegetation effects on the microwave emission of soils. *Remote Sensing of Environment*, *36*, 203—212.

Jarvis, P. G. (1976). The interpretation of the variations in leaf water potential and stomatal conductance found in canopies in the field. *Philosophical Transactions of the Royal Society of London, Series B*, *273*, 593—610.

Jiang, L., & Islam, S. (2003). An intercomparison of regional latent heat flux estimation using remote sensing data. *International Journal of Remote Sensing*, *24*, 2221—2236.

Kosugi, Y. (1996), Leaf-scale analysis of the CO2 and H2O exchange process between trees and atmosphere, Ph.D. dissertation, Kyoto Univ., Kyoto, Japan,

Lin, B., & Minnis, P. (2000). Temporal variations of land surface microwave emissivities over the ARM southern great plains site. *Journal of Applied Meteorology*, *39*, 1103—1116.

Lin, B., Minnis, P., Fan, A., Curry, J., & Gerber, H. (2001). Comparison of cloud liquid water paths derived from in situ and microwave radiometer data taken during the SHEBA/FIREACE. *Geophysical Research Letters*, *28*, 975—978.

Lin, B., Wielicki, B., Minnis, P., & Rossow, W. B. (1998). Estimation of water cloud properties from satellite microwave, infrared, and visible measurements in oceanic environments. I: Microwave brightness temperature simulations. *Geophysical Research Letters*, *103*, 3873—3886.

McClathey, R. A., Fenn, R. W., Selby, J. E. A., Voltz, F. E., & Garing, J. S. (1972). *Optical properties of the atmosphereEnvironmental Research Papers*, *vol. 411*. Air Force Cambridge Research Laboratories AFCRL-72-0497.

Min, Q. (2005). Impacts of aerosols and clouds on forest–atmosphere carbon exchange. *Journal of Geophysical Research*, *110*. doi:10.1029/2004JD004858. D06203.

Min, Q., & Lin, B. (2006). Remote sensing of evapotranspiration and carbon uptake at Harvard forest. *Remote sensing of environment*, *100*, 379—387.

Min, Q., & Lin, B. (2006). Determination of spring onset and growing season leaf development using satellite measurements. *Remote sensing of environment*, *104*, 96—102.

Min, Q., & Wang, S. (2008). Clouds modulate terrestrial carbon uptake in a midlatitude hardwood forest.*Geophysical Research Letters*, *35*. doi:10.1029/2007GL032398. L02406.

Monteith, J. L. (1995). Accommodation between transpiring vegetation and the convective boundary layer. *Journal of Hydrology*, *166*, 251—263.

Moore, K. E., Fitzjarald, D. R., Sakai, R. K., Goulden, M. L., Munger, J. W., & Wofsy, S. C. (1996). Seasonal variation in radiative and turbulent exchange at a deciduous forest in Central Massachusetts. *Journal of Applied Meteorology*, *35*, 122—134.

Myneni, R. B., Hall, F. G., Sellers, P. J., & Marshak, A. L. (1995). The interpretation of spectral vegetation indexes. *IEEE Transactions on Geoscience and Remote Sensing*, *33*, 481—486.

Nishida, K., Nemani, R. R., Running, S. W., & Glassy, J. M. (2003). An operational remote sensing algorithm of land surface evaporation. *Journal of Geophysical Research*, *108* (D9), 4270. doi:10.1029/2002JD002062.

Njoku, E. G., & Li, L. (1999). Retrieval of land surface parameters using passive microwave measurements at 6–18 GHz. *IEEE Transactions on Geoscience and Remote Sensing*, *37*, 79—93.

O'Brien, K. L. (1996). Tropical deforestation and climate change. *Progress in Physical Geography*, *20*, 311—335.

Priestley, C. H. B., & Taylor, R. J. (1972). On the assessment of surface heat flux and evaporation using large-scale parameters. *Monthly Weather Review*, *100*, 81—92.

Sellers, P. J. (1985). Canopy reflectance, photosynthesis and transpiration. *International Journal of Remote Sensing*, *6*, 1335—1372.

Shukla, J., & Mintz, Y. (1982). Influence of land-surface evapotranspiration on the Earth's climate. *Science*, *215*, 1498—1501.

Shukla, J., Nobre, C., & Sellers, P. (1990). Amazon deforestation and climate change. *Science*, *247*, 1322—1325.

Shuttleworth, W. J., Gurney, R. J., Hsu, A. Y., & Ormsby, J. P. (1989). *FIFE: The variation in energy partition at surface flux sites*, *vol. 186*. (pp. 67—74): IAHS Publication.

Wang, J., Chagnon, F. J. F., Williams, E. R., Betts, A. K., Renno, N. O., Machado, L. A. T., et al. (2009). Impacts of deforestation in the Amazon basin on cloud climatology. *PNAS*, *106*, 3670—3674.

Wofsy, S. C., Goulden, M. L., Munger, J. W., Fan, S. M., Bakwin, P. S., Daube, B. C., et al. (1993). Net exchange of CO2 in midlatitude forests. *Science*, *260*, 2224—2238.

Zeng, N., Neelin, J. D., Lau, K. M., & Tucker, C. J. (1999). Enhancement of interdecadal climate variability in the Sahel by vegetation interaction. *Science*, *286*, 1537—1540.